The new physics of non-equilibrium condensates: insights from classical dynamics

2007 J. Phys.: Condens. Matter 19 295210

(http://iopscience.iop.org/0953-8984/19/29/295210)

IOP PUBLISHING JOURNAL OF PHYSICS: CONDENSED MATTER

J. Phys.: Condens. Matter **19** (2007) 295210 (10pp) doi:10.1088/0953-8984/19/29/295210

The new physics of non-equilibrium condensates: insights from classical dynamics

P R Eastham

Theory of Condensed Matter, Cavendish Laboratory, Cambridge CB3 0HE, UK

Received 17 April 2007
Published 11 June 2007
Online at stacks.iop.org/JPhysCM/19/295210

Abstract

We discuss the dynamics of classical Dicke-type models, aiming to clarify the mechanisms by which coherent states could develop in potentially non-equilibrium systems such as semiconductor microcavities. We present simulations of an undamped model which show spontaneous coherent states with persistent oscillations in the magnitude of the order parameter. These states are generalizations of superradiant ringing to the case of inhomogeneous broadening. They correspond to the persistent gap oscillations proposed in fermionic atomic condensates, and arise from a variety of initial conditions. We show that introducing randomness into the couplings can suppress the oscillations, leading to a limiting dynamics with a time-independent order parameter. This demonstrates that non-equilibrium generalizations of polariton condensates can be created even without dissipation. We explain the dynamical origins of the coherence in terms of instabilities of the normal state, and consider how it can additionally develop through scattering and dissipation.

1. Introduction

Cavity polaritons [1–5] are the quanta of the electromagnetic field in a semiconductor microcavity. Since they are part photon, cavity polaritons are bosons. Thus there is the possibility of forming a Bose condensate of polaritons, in which an incoherent population of polaritons becomes coherent due to the combined effects of bosonic statistics and interactions. The last few years have seen a steady accumulation of evidence for such physics. Initial observations of a threshold [6, 7] in the intensity of the emitted light as a function of pumping power have been supplemented by demonstrations of both temporal [8] and spatial [9] coherence in the emission. Evidence that the phenomenon is not conventional lasing includes the persistence of polaritonic features in the spectrum above threshold: a polaritonic spectrum arises from a coherent polarization in the gain medium, while such polarization is negligible in conventional laser theory.

One route to developing theories of polariton condensation is to begin with the quasi-equilibrium limit of a population of polaritons. The established techniques of many-particle

physics can then be applied to model microcavities, and theories developed which allow for issues such as the internal structure of the polaritons, disorder acting on the excitons, and the many-body nature of Bose condensation. This approach has now established phase diagrams and observable properties for polariton condensation in a range of increasingly realistic models [10–20].

The problem with the equilibrium theories is linking them to the experiments, which may not be in thermal equilibrium. In principle they are directly applicable if the polariton lifetime is long compared with the thermalization time. Unfortunately, while the polariton lifetime is easily established to be of the order of picoseconds, it is difficult to get a handle on the thermalization time. In practice the typical situation appears to be that the system does not thermalize below the nonlinear threshold, but can do above it [21]. Thus while equilibrium theories are apparently sometimes directly applicable to the condensed state, further work is needed to understand the threshold itself, and the apparent equilibration below it.

Polariton condensation experiments are one topical motivation for reconsidering a fundamental issue in the physics of coherent many-particle states: the origins of the coherence. Since in equilibrium the coherent state is selected because it has a lower energy than the incoherent state, one might expect the origins of coherence to be in dissipation and thermalization. Yet coherence can develop in the absence of dissipation (e.g. superradiance) or in dissipative systems that are not in thermal equilibrium (e.g. lasing and the non-equilibrium condensation proposed in [22]).

There are many areas beyond polariton condensation where the origins of coherence are relevant. In microcavities one has access to a range of non-equilibrium states, created for example by coherent pumping [23], and hence a laboratory for widely exploring mechanisms which create and preserve coherence. In atomic Bose gases the development of condensates has been studied both theoretically and experimentally [24–26], and there has been much recent interest in non-adiabatic phenomena involving coherent states of atomic Fermi gases [27–29].

In this paper we explore the origins of coherence by discussing the dynamics of classical Dicke-type models. We first consider an undamped model, which we present in section 2 along with a brief review of some analytical results on its dynamics. In section 3 we then present and discuss some numerical simulations showing that some of the coherent steady states are reached from some initial conditions, even in the absence of dissipation. In section 4 we explain, in terms of the dynamical stability of the incoherent states, why this occurs. In a special case of the model the results can be further understood using exact solutions, as we discuss in section 5. In section 6 we discuss a phenomenological approach to adding damping to the dynamics, and present numerical results showing the approach to an equilibrium condensate. Finally, in section 7 we propose several scenarios for how coherence could develop in a polariton condensation experiment, and summarize our conclusions.

2. Background and basic model

The basic model we consider here directly describes excitons strongly localized on disorder in a three-dimensional cavity. It has the Hamiltonian

$$H = \omega_c \psi^\dagger \psi + \sum_i \left[E_i S_i^z + \frac{g_i}{\sqrt{N}} \left(S_i^+ \psi + \psi^\dagger S_i^- \right) \right]. \tag{1}$$

$\psi^\dagger$ is the creation operator for a cavity photon, with energy ω_c. The dielectric is modelled as a set of N two-level systems, with the ith two-level system described by the spin-half operators $\vec{S}_i$. The eigenstates of S_i^z correspond to the presence or absence of an excitation on site i.

The form of (1) is a generalization of the well-known Dicke model to include a distribution of exciton energies (i.e. inhomogeneous broadening) and coupling strengths. It is one of the central models of quantum optics, describing for example lasing [30], equilibrium superradiance [31] and dynamical superradiance [32]. It can be viewed as a generalization of the BCS Hamiltonian to the strong-coupling regime, as is apparent on rewriting the spin operators in terms of two species of fermions. It was applied to polariton condensation by Eastham and Littlewood [10–12], who considered its quasi-equilibrium thermodynamics at fixed excitation number

$$L = \psi^\dagger \psi + \sum_i S_i^z; \tag{2}$$

note this is conserved by (1). The resulting polariton condensate can be viewed as a generalization of the BCS state to include coherent photons. Later work on the equilibrium polariton condensate in models of the basic form (1) includes generalizations to include propagating photons [16, 17], decoherence [14] and more realistic approaches to disorder [15, 19]. The same theoretical framework has also been applied to condensation in atomic gases of fermions [33, 34].

To study the dynamics of the model (1) we begin from the Heisenberg equations of motion for the operators. However, we shall not consider the full quantum dynamics described by these equations. Instead we consider the simpler problem obtained by replacing the operators in the equations of motion with classical variables. This is equivalent to taking the expectations of the equations of motion and approximating the expectation values of products as products of expectation values. Thus we consider a mean-field dynamics for the quantum model. Since mean-field theory is exact for the thermodynamics in the limit $N \to \infty$ we expect it to account for many features of the dynamics when N is large.

Thus the classical equations of motion we consider are

$$\mathrm{i}\dot{\psi} = \omega_\mathrm{c}\psi + \frac{1}{2\sqrt{N}} \sum_i g_i \sigma_i^-, \tag{3a}$$

$$\dot{\vec{\sigma}}_i = \vec{\sigma}_i \times \vec{B}_i, \tag{3b}$$

$$\vec{B}_i = (-2g_i \,\mathrm{Re}(\psi)/\sqrt{N}, 2g_i \,\mathrm{Im}(\psi)/\sqrt{N}, -E_i), \tag{3c}$$

where $\vec{\sigma}_i/2 = \vec{S}_i$ and $\sigma_i^- = \sigma_i^x - \mathrm{i}\sigma_i^y$.

We shall describe the model as having excitonic coherence if the phases of the different σ_i^- are correlated. Equivalently, the xy components of the total spin vector, $\vec{\sigma}_T = \sum_i \vec{\sigma}_i$, are of order N. This leads, according to (3*a*), to a state with $\psi \sim \sqrt{N}$.

2.1. Steady-state solutions

In previous work [35] we identified two classes of steady-state solutions to (3*a*)–(3*c*) when $N \to \infty$. The simplest class consists of solutions in which there is no excitonic coherence and a cavity field of order N^0. In this case as $N \to \infty$ the spin i freely precesses around the z-axis at its natural frequency E_i, so the excitons remain incoherent and the solution is self-consistent. These solutions are generalizations of the normal state in the equilibrium theory. When N is finite but large there is a subset of such solutions which remain incoherent, including at least those where the cavity field and excitonic polarization are exactly zero.

The second class consists of synchronized steady states which generalize the condensed solutions of the equilibrium theory. In these states there is an $\mathrm{O}(\sqrt{N})$ component to ψ oscillating at a single frequency, $\psi \sim \lambda\sqrt{N}\mathrm{e}^{-\mathrm{i}\mu t}$. In a frame rotating at this frequency the spin dynamics for large N is just free precession about a static effective field

$\tilde{\vec{B}}_i = (-2g_i\,\mathrm{Re}(\lambda), 2g_i\,\mathrm{Im}(\lambda), -(E_i-\mu))$. Incorporating this dynamics in (3*a*), we find that the leading-order terms are satisfied if

$$(\omega_c-\mu)\lambda = \frac{\lambda}{N}\sum_i \frac{g_i^2\sigma_i^{z\prime}(0)}{\sqrt{(E_i-\mu)^2+4g_i^2|\lambda|^2}}. \tag{4}$$

Here $\sigma_i^{z'}(0)$ denotes the initial component of the ith spin along its effective field $\tilde{\vec{B}}_i$. If every spin lay parallel to its effective field $\tilde{\vec{B}}_i$ then (4) would be the gap equation for the polariton condensate at $T=0$, but we see that there are many more self-consistent solutions with non-equilibrium distributions of $\sigma_i^{z'}(0)$.

We note that the self-consistency argument admits the possibility of steady states where the spins do not lie along their effective fields, because the dominant terms in the sum on the right of (3*a*) come from components of σ^- which oscillate at frequency μ. If the spins do not lie along $\tilde{\vec{B}}_i$ then there are additional components at frequencies $\mu \pm |\tilde{\vec{B}}_i|$, but since these frequencies differ for each spin they give terms of O(1) in (3*a*). Thus these components are irrelevant when $N\to\infty$. For N finite but large they lead to noise sources which drive the O(1) component of ψ, and so would not change the macroscopic behaviour so long as the states are dynamically stable.

2.2. *Exact solutions*

In recent work [36], the non-equilibrium gap equation (4) is derived from an exact solution to the model (3*a*)–(3*c*). This solution applies to the special case $g_i = g$ in which the model is integrable. A similar equation is also given for the steady states of the BCS model in [37]. The exact solutions go well beyond the arguments above, and show that there are many further classes of solutions in which $|\psi|$ oscillates with a small number of frequencies. The next simplest solutions correspond to an ansatz proposed by Barankov and Levitov [38], and have oscillations of the order parameter described by elliptic functions. An approach for determining the type of solution which evolves from a given initial condition is discussed in [39], and can be applied to the Dicke model using the Lax vector given in [36].

3. Numerical results

Having seen that the model (3*a*)–(3*c*) has coherent solutions, we now consider whether the coherence can develop dynamically when N is finite but large. This question can, for the integrable model $g_i = g$, be analysed entirely using the exact solutions. We shall approach it instead through numerical solutions to the equations of motion, allowing us to go beyond the exactly solved model, and return to discuss how the results link to the exact solution in section 5.

We first consider the model when $g_i = g$, and choose our units of energy such that $g = 2$, and the zero of energy such that $\omega_c = 0$. We take the energies to be drawn from a Gaussian of standard deviation $\sigma = 0.3$ and mean zero, so the photons are resonant with the centre of the inhomogeneously broadened exciton line.

The dynamics in general depends on the initial conditions. We consider initial conditions in which there is no correlation between the spin and energy on each site. To construct an initial condition with negligible classical coherence we take the spins to make angles to the z-axis chosen from a uniform distribution over $[\theta_1, \theta_2]$, and to have angles to the x-axis drawn from a uniform distribution over $[0, 2\pi]$. Since we are looking for symmetry-broken solutions we also include a small initial seed for the cavity field.

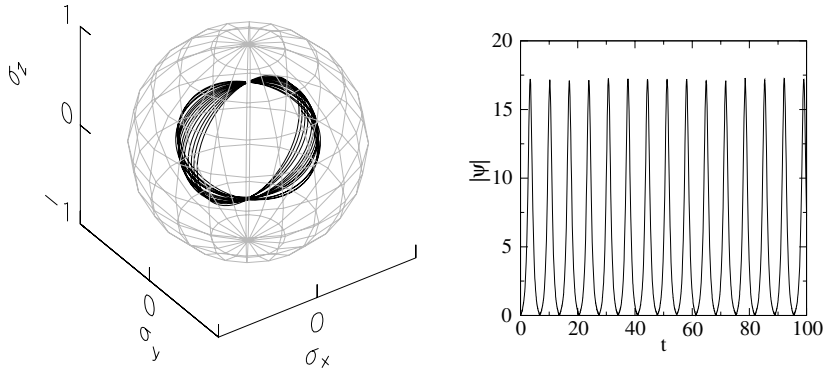

Figure 1. Locus of the total spin vector to $t = 100$ (left panel) and cavity mode amplitude (right panel) for the classical Dicke model with $g_i = g = 2$ and $N = 500$, starting in an unphased inverted initial condition. $\omega_c = 0$ and the energies E_i are drawn from a Gaussian with mean 0 and standard deviation 0.3. The initial state has a small photon field and spins whose angles to the $z(x)$-axis are drawn uniformly from $[0, \pi]([0, 2\pi])$.

For this type of initial condition our simulations of the dynamics do not develop coherent photons unless the average $\sigma_i^z(0)$ exceeds a positive threshold. An example of the behaviour when it does is shown in figure 1, for 500 spins with $\theta_1 = 0$ and $\theta_2 = \pi/2$. The left panel shows the locus of the tip of the total spin vector $\vec{\sigma}_T/N$ up to $t = 100$. The right panel shows the associated field amplitude $|\psi|$. The behaviour contrasts with that obtained in a simulation starting from non-inverted initial conditions, $\sigma_T^z(0)/N < 0$, and shown in the left panel of figure 4. In this case the locus becomes a point as $N \to \infty$, and the photon field remains of O(1).

As can be seen from figure 1, there are mechanisms in the Dicke model that can generate coherence from an incoherent state, even without dissipation. However, for this class of initial conditions they are only effective in inverted states, whereas equilibrium condensation does not require inversion. A more immediately obvious relation is to strong-coupling superradiant dynamics, demonstrated experimentally in [40]. This phenomenon can be treated by considering the classical Dicke model with $E_i = E$ and $g_i = g$, so that (3*a*)–(3*c*) reduce to equations for ψ and $\vec{\sigma}_T$. The dynamics of $\vec{\sigma}_T$ can then be shown to be that of a rigid pendulum [41]. Since the length of $\vec{\sigma}_T$ is conserved when $E_i = E$ the excitonic system must become coherent if the pendulum swings towards the equator. The 'gravity' on this pendulum acts down in figure 1, so that coherence increases only from inverted states. This asymmetry in the dynamics is ultimately due to the rotating-wave approximation made in (1), which defines directions of energy flow between the cavity mode and exciton.

In the absence of a field the polarization of an initially coherent state undergoes free induction decay, as the different two-level systems go out of phase due to the inhomogeneous broadening. An interesting feature of figure 1 is that the coherence does not appear to decay even in the presence of an inhomogeneous broadening. Such undamped dynamics for the cavity mode is reminiscent of self-induced transparency [42], in which soliton-like pulses propagate unattenuated in an inhomogeneously broadened medium.

It becomes possible to generate spontaneous coherence in the Hamiltonian dynamics without inversion if one considers initial conditions in which the spins are correlated with energy. In particular, Barankov and Levitov recently presented an ansatz [38] which solves the dynamics starting from a Fermi sea. In these solutions there is a coherent cavity field whose amplitude undergoes undamped oscillations like those in figure 1. As we will discuss

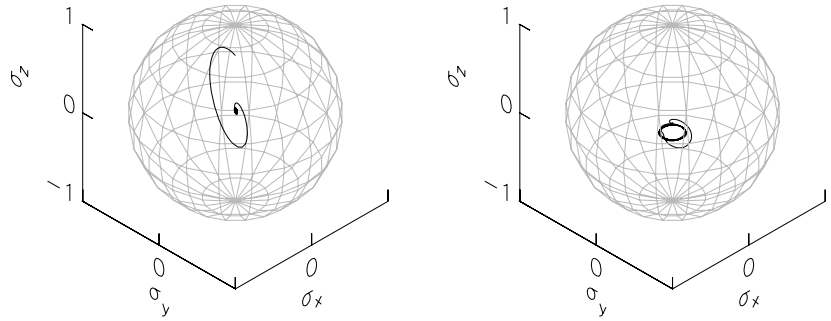

Figure 2. Destruction of the gap oscillations by a distribution of g. Left panel: parameters of figure 1 except that $N = 2000$ and g is drawn from a Gaussian of mean 2 and standard deviation 0.6. Right panel: same parameters starting from a Fermi sea with a Fermi energy 0.05 below the centre of the inhomogeneously broadened exciton line.

in section 5, the coherent dynamics we find in simulations corresponds to the solution given in [38], although our initial conditions are not considered there.

Although the oscillations are not suppressed by randomness in E_i, it appears that they can be suppressed by randomness in the coupling constants g_i, which exists in a disordered semiconductor [19]. The left panel of figure 2 shows the dynamics in the Bloch sphere for the same parameters as figure 1, but with the coupling constants now drawn from a Gaussian with mean 2 and standard deviation 0.6. The right panel shows the results for the same parameters but starting from a Fermi sea with the Fermi edge at an energy 0.05 below the middle of the band; without the randomness of g this initial condition results in persistent gap oscillations. In both cases we see that the oscillations of the macroscopic electromagnetic field, which according to (2) correspond to oscillations in σ_T^z, disappear at late times. The dynamics reaches a steady-state condensate with a uniform field, corresponding to the self-consistency condition (4). Starting from an inverted, uncorrelated state the final solution appears to be the trivial one in which the locking frequency $\mu = \omega_c$ and there is no coherent polarization: the two-level systems are in a dephased state, which has decoupled from a residual cavity field developed during the early stages of the dynamics. Starting from a Fermi sea, however, we see that the late-time attractor of the dynamics is a circle: it has reached non-trivial locked states in which the locking frequency differs from ω_c and there is therefore a coherent excitonic polarization.

4. Linear stability analysis

A simple way to understand why either inversion or a Fermi sea allows coherence to develop is to consider a linear stability analysis of the incoherent state. The action for fluctuations around the incoherent thermal equilibrium state is equation (23) in [11], so the real eigenfrequencies λ are the solutions to

$$\omega_c - \lambda - \frac{1}{N}\sum_i \frac{g_i^2 \tanh(\beta\tilde{E}_i/2)}{E_i - \lambda} = 0, \tag{5}$$

where $\tilde{E}_i$ is E_i measured from the chemical potential for polaritons. More generally one can linearize the zero-temperature dynamics about an arbitrary normal state [38, 43], which corresponds to replacing the thermal equilibrium $\sigma_i^z = -\tanh(\beta\tilde{E}_i/2)$ in (5) with the general $\sigma_i^z(0)$ of the non-equilibrium state:

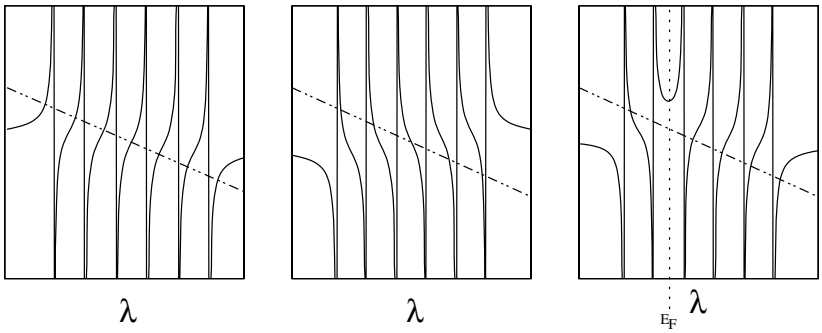

Figure 3. Illustration of the left (dot–dashed) and right (solid) sides of equation (6), determining the eigenfrequencies λ of the normal state. Left panel: stable incoherent state with σ_i^z independent of energy and less than zero. Middle panel: unstable incoherent state with σ_i^z independent of energy and greater than zero. Right panel: unstable Fermi sea, $\sigma_i^z = +(-)1$ for $E_i < (>)E_F$.

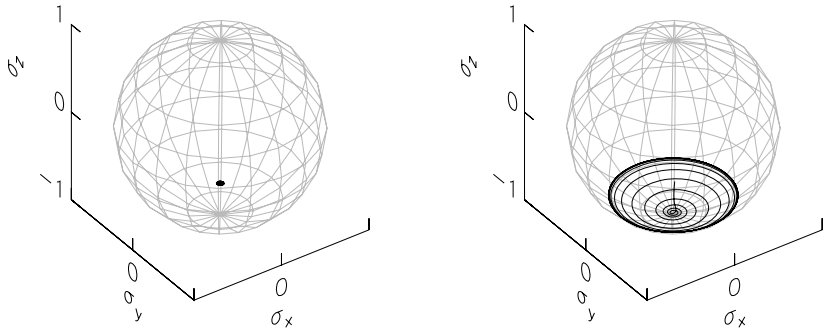

Figure 4. Locus of the total spin vector up to $t = 100$ starting from an initial condition where the spins have angles to the x-axis chosen uniformly from $[0, 2\pi]$, and to the z-axis from $[\pi, 2\pi]$. Left panel: undamped model. Right panel: model with phenomenological damping $\gamma = 1$. $N = 2000$, E_i from a Gaussian with mean 1 and standard deviation 0.5, $g_i = g = 2$, $\omega_c = 1$.

$$\omega_c - \lambda = -\frac{1}{N}\sum_i \frac{g_i^2 \sigma_i^z(0)}{E_i - \lambda}. \tag{6}$$

In passing we note that the analogous generalization of the thermodynamic action for fluctuations about the condensate, equation (22) of [11], gives the eigenspectrum for the coherent steady states with a uniform gap and every spin parallel or antiparallel to its effective field, but more generally there are additional terms generated by the components of the spins transverse to the effective fields.

A dynamical instability is indicated by the appearance of a complex root in (6). In figure 3 we plot the left and right sides of (6) for real λ, a small number $N = 6$ of two-level systems, and three types of initial states. For an uncorrelated non-inverted state (left panel) there are $N + 1$ real roots which generalize the inhomogeneously broadened polariton spectrum to the non-equilibrium states. When g becomes large compared with the bandwidth the two poles outside the band correspond to the usual upper and lower polariton, with a band of $N - 1$ almost excitonic states between them. The instability of an uncorrelated inverted state is shown in the middle panel. We see that the two 'polariton' roots can become complex, indicating the superradiant instability.

For completeness we illustrate the instability of a Fermi sea in the right panel. The sign change in $\sigma_i^z(0)$ across the Fermi energy introduces a turning point in the right-hand side of (6). At $T = 0$ there can be a stable Fermi sea in the finite system, which has two 'excitonic' roots near the Fermi edge. These roots become complex at the instability, which can be reached by increasing the system size or changing the detuning. At this instability pairs of exciton states either side of the Fermi edge begin to develop a polarization. The generalization to a Fermi distribution in the thermodynamic limit is clear: if the distribution has a sharp enough step, i.e. the temperature is low enough, there can be an instability.

5. Exact solutions

In the case $g_i = g$ the model we have considered is exactly solvable, and its solution is equivalent to that of the BCS model [36]. The linear stability analysis above can be extended by linking it to the exact solutions through the concept of the Lax vector. In our notation the Lax vector $\vec{L}(u)$ for the generalized Dicke model with $g_i = g$ is [36]

$$\tilde{\vec{L}}(u) = \frac{g^2}{N}\vec{L}(u) = \begin{pmatrix} 2g\,\mathrm{Re}\,(\psi)/\sqrt{N} \\ -2g\,\mathrm{Im}\,(\psi)/\sqrt{N} \\ 2u - \omega_c \end{pmatrix} + \frac{g^2}{N}\sum_i \frac{\vec{\sigma}_i}{2u - E_i}. \tag{7}$$

As discussed in [39], the character of the dynamics is connected to the number of isolated branch cuts of the conserved function $\sqrt{\vec{L}^2(u)}$. For a single cut the long-time dynamics has a constant order parameter obeying (4), while for two cuts one obtains the oscillating gap solution [38]. The particular parameters within each class of solution, such as order parameters and the locking frequencies, depend on the initial conditions.

For incoherent initial conditions $\tilde{\vec{L}}(\vec{u}) = \vec{k}L_z(u) + \vec{L}_{xy}(u)$ lies almost parallel to $\vec{k}$. Comparing (7) with (6) we see that the zeroes of $L_z(u)$ and the eigenfrequencies of the linear stability analysis are related as $2u = \lambda$. Thus for the stable case in the left panel of figure 3 the zeros of $L_z(u)$ lie along the real axis, while in the unstable cases shown there are two complex conjugate roots off the axis. All these roots lead to doubly degenerate roots of $L_z^2(u)$, which are then split by the perturbation $\vec{L}_{xy}$. Thus the unstable states we consider have two isolated branch cuts, and thus correspond to the oscillating gap solution.

6. Damping

We have discussed two dynamical mechanisms for creating coherence in the undamped Dicke model: an instability of the polariton-like modes which occurs from inverted initial states, and an instability at the Fermi edge which occurs from a low-temperature Fermi distribution. However, since the polariton condensate is the thermal equilibrium state then at low enough temperatures the mechanisms which establish thermal equilibrium, i.e. dissipation and scattering, must somehow generate coherence.

A simple phenomenological way to extend the Dicke model to include dissipation is to add a term $-\gamma\vec{\sigma}_i \times (\vec{\sigma}_i \times \vec{B}_i)$ to the right of (3*b*). By construction such a term tends to align each spin with its effective field $\vec{B}_i$. However, the effective field $\vec{B}_i$ depends on the choice of rest frame, i.e. the zero of energy. In the equilibrium case the spins align with their effective fields in the rest frame of the chemical potential. Thus we see that with the damping term implicitly introduces a chemical potential, and is associated with equilibration with an exciton bath.

In the right panel of figure 4 we illustrate the approach to an equilibrium condensate under phenomenological damped dynamics. The initial state here has spins randomly oriented in

the southern hemisphere of the Bloch sphere, and does not develop coherence without the damping term. The damping term acts to align the phases of the exitons and generate a coherent state. The final locking frequency of the condensate for these parameters is approximately the equilibrium chemical potential $\mu_{\rm pol}$ which gives the steady-state value of L; it comes closer still in simulations with smaller damping terms. $\mu_{\rm pol}$ is not in general identical to the chemical potential $\mu_{\rm ex}$ implied by the choice of rest frame because the former is coupled to both excitons and photons and the latter only to excitons.

7. Conclusions and outlook

In a polariton condensation experiment a microcavity is pumped at high energies, while with sufficiently strong pumping coherent polaritons are observed at low energies. A first approximation to this situation treats the pumping as a high-energy exciton reservoir which randomly populates the low-energy excitons independently of their energy. Within this approximation we can suggest several scenarios, differentiated by the relative timescales for thermalization, exciton decay and photon decay, which would lead to coherent photons.

If thermalization and exciton decay are negligible we expect a scenario which might be described as a 'polariton laser'. The reservoir will build up the inversion until the superradiance threshold is exceeded, and the dynamical instability serves to create a coherent photon field. This then opens a decay channel allowing the excitation L to decay through the photons, which for a large reservoir is expected to result in a stationary value of L produced by competition between pumping and damping.

If thermalization occurs before the excitons decay, and to a low enough temperature, we could have an analogous scenario but with the coherence developing before the superradiance threshold. Conceptually the coherence could develop either through the creation of a Fermi edge and the resulting dynamical instability or directly through dissipation, but in practice these are intimately related.

In conclusion, we have illustrated both dissipative and non-dissipative mechanisms which generate coherence from incoherent initial states in Dicke-type models. These include polaritonic and pairing instabilities, which we have seen generating solutions with both oscillating and static ordering, and a phenomenological dissipation mechanism which generates the equilibrium condensate solution. The non-dissipative mechanisms only lead to coherent solutions from specific initial conditions. Within the classes of initial conditions we have considered it appears from our simulations that either inversion, a Fermi edge, or dissipation are needed to generate coherence.

Acknowledgments

I acknowledge helpful discussions with Peter Littlewood, Jonathan Keeling, Ben Simons and Francesca Marchetti. This work is supported by the EPSRC, Sidney Sussex College and the EU network 'Photon-mediated phenomena in semiconductor nanostructures'.

References

[1] Hopfield J J 1958 *Phys. Rev.* **112** 1555
[2] Weisbuch C, Nishioka M, Ishikawa A and Arakawa Y 1992 *Phys. Rev. Lett.* **69** 3314
[3] Skolnick M S, Fisher T A and Whittaker D M 1998 *Semicond. Sci. Technol.* **13** 645
[4] Savona V 1999 *Confined Photon Systems* (*Springer Lecture Notes in Physics*) ed H Benisty, J-M Gérard, R Houdré, J Rarity and C Weisbuch (Berlin: Springer) p 173

[5] Kavokin A and Malpuech G 2003 *Cavity Polaritons* (*Thin Films and Nanostructures* vol 32) (Amsterdam: Elsevier)
[6] Dang L S, Heger D, André R, Bœuf F and Romestain R 1998 *Phys. Rev. Lett.* **81** 3920
[7] Senellart P and Bloch J 1999 *Phys. Rev. Lett.* **82** 1233
[8] Deng H, Weihs G, Snoke D, Bloch J and Yamamoto Y 2003 *Proc. Natl Acad. Sci.* **100** 15318
[9] Richard M, Kasprzak J, Romestain R, André R and Dang L S 2005 *Phys. Rev. Lett.* **94** 187401
[10] Eastham P R and Littlewood P B 2000 *Solid State Commun.* **116** 357
[11] Eastham P R and Littlewood P B 2001 *Phys. Rev.* B **64** 235101
[12] Eastham P R 2000 *Bose Condensation in a Model Microcavity PhD Thesis* University of Cambridge
[13] Szymanska M H and Littlewood P B 2002 *Solid State Commun.* **124** 103
[14] Szymanska M H, Littlewood P B and Simons B D 2003 *Phys. Rev.* A **68** 013818
[15] Marchetti F M, Simons B D and Littlewood P B 2004 *Phys. Rev.* B **70** 155327
[16] Keeling J, Eastham P R, Szymanska M H and Littlewood P B 2004 *Phys. Rev. Lett.* **93** 226403
[17] Keeling J, Eastham P R, Szymanska M H and Littlewood P B 2005 *Phys. Rev.* B **72** 115320
[18] Marchetti F M, Szymanska M H, Eastham P R, Simons B D and Littlewood P B 2005 *Solid State Commun.* **134** 111
[19] Marchetti F M, Keeling J, Szymanska M H and Littlewood P B 2005 *Phys. Rev. Lett.* **96** 066405
[20] Eastham P R and Littlewood P B 2006 *Phys. Rev.* B **73** 085306
[21] Richard M, Kasprzak J, André R, Romestain R, Dang L S, Malpuech G and Kavokin A 2005 *Phys. Rev.* B **72** 201301
[22] Szymanska M H, Keeling J and Littlewood P B 2006 *Phys. Rev. Lett.* **96** 230602
[23] Baumberg J J, Savvidis P G, Stevenson R M, Tartakovskii A I, Skolnick M S, Whittaker D M and Roberts J S 2000 *Phys. Rev.* B **62** R16247
[24] Stoof H T C 1995 *Bose Einstein Condensation* ed A Griffin, D W Snoke and S Stringari (Cambridge: Cambridge University Press) p 226
[25] Köhl M, Davis M J, Gardiner C W, Hansch T and Esslinger T 2002 *Phys. Rev. Lett.* **88** 080402
[26] Davis M J and Gardiner C W 2002 *J. Phys.* B **35** 733
[27] Barankov R and Levitov L S 2006 *Phys. Rev. Lett.* **96** 230403
[28] Yuzbashyan E A and Dzero M 2006 *Phys. Rev. Lett.* **96** 230404
[29] Szymanska M H, Simons B D and Burnett K 2005 *Phys. Rev. Lett.* **94** 170402
[30] Haken H 1975 *Rev. Mod. Phys.* **47** 67
[31] Hepp K and Lieb E H 1973 *Ann. Phys.* **76** 360
[32] Dicke R H 1954 *Phys. Rev.* **93** 99
[33] Holland M, Kokkelmans S J J M F, Chiofalo M L and Walser R 2001 *Phys. Rev. Lett.* **87** 120406
[34] Timmermans E, Furuya K, Milonni P W and Kerman A K 2001 *Phys. Lett.* A **285** 228
[35] Eastham P R, Szymanska M H and Littlewood P B 2003 *Solid State Commun.* **127** 117
[36] Yuzbashyan E A, Kuznetsov V B and Altshuler B L 2005 *Phys. Rev.* B **72** 144524
[37] Barankov R A and Levitov L S 2006 *Phys. Rev.* A **73** 033614
[38] Barankov R A and Levitov L S 2004 *Phys. Rev. Lett.* **93** 130403
[39] Yuzbashyan E A, Tsyplyatyev O and Altshuler B L 2006 *Phys. Rev. Lett.* **96** 097005
Yuzbashyan E A, Tsyplyatyev O and Altshuler B L 2006 *Phys. Rev. Lett.* **96** 179905 (erratum)
[40] Kaluzny Y, Goy P, Gross M, Raimond J M and Haroche S 1983 *Phys. Rev. Lett.* **51** 1175
[41] Bonifacio R and Preparata G 1970 *Phys. Rev.* A **2** 336
[42] McCall S L and Hahn E L 1969 *Phys. Rev.* **183** 457
[43] Littlewood P B and Zhu X 1996 *Phys. Scr.* T **68** 56